WORLD CONFERENCE ON TIMBER ENGINEERING 2025
BRISBANE, AUSTRALIA
Advancing Timber for the Future Built Environment

FEASIBILITY OF CROSS-LAMINATED TIMBER PANEL FOR BRIDGES APPLICATION: PRELIMINARY EXPERIMENTAL, NUMERICAL AND ANALYTICAL STUDY

Reza Masoundia[1]

ABSTRACT: Application of CLT in both structural and non-structural elements of bridges has increased globally. The CLT panel comprises several layers of timber boards which are stacked crosswise at 90 degrees and glued together on the wider face of timber boards. Although CLT panel has played a significant role in the current progress of timber mass construction in Pasefic area, there is not even one notable bridge CLT project. Therefore, this paper investigates the feasibility of using CLT panels in bridge applications, based on local material. This research examines the structural performance of CLT experimentally, numerically, and analytically. Experimental test results demonstrate that CLT and CLT composite double T-beams are sufficiently strong to carry structural loads for bridge applications. A numerical parametric study, based on an experimentally verified ABAQUS model, confirmed that a bare CLT panel and CLT composite elements which are fabricated from locally grown Radiata Pine are structurally ideal for short to intermediate span bridge application. This study revealed that the CLT bridge has potential for factory prefabrication which makes site assembly faster. Additionally, majority of non-structural bridge elements could be supplied from wasted CLT material. Ultimately, the CLT bridge is an excellent, environmentally friendly alternative to concrete bridges with a lower environmental impact.

KEYWORDS: CLT, Bridge, CLT composite, Numerical study, Prefabrication.

1- INTRODUCTION

Cross-laminated timber (CLT) panels offer potential for a wide range of structural applications, including timber bridges. While CLT is still a relatively new material in bridge construction, it has become increasingly popular in residential and commercial building projects [1–6].

CLT is a high-performance, solid engineered wood product, generally manufactured from low-grade softwood species like Radiata Pine. These layers are bonded together in a crosswise arrangement. CLT panels usually have a symmetrical layup, with standard thicknesses ranging from 126 mm to 420 mm, and typically comprise three to eleven layers (refer to Figure 1) [1–6].

New Zealand produces a significant volume of timber each year, with Radiata Pine making up approximately 90% of its plantation forests. This species is favored due to its relatively short rotation period (25–30 years) and high timber productivity. Well-managed sites can yield quality timber at rates of 30 m³/ha/year, and up to 50 m³/ha/year [5,11].

CLT panels offer numerous advantages including design flexibility, quick installation, and strong seismic performance which have supported their growing use in different structural forms, from buildings to bridges. Furthermore, a cost-effectiveness study conducted in the United States has shown that CLT structures are competitively priced when compared to concrete, masonry, and steel alternatives [7–9].

Although numerous studies have been conducted on concrete-steel composite bridges, there is still a lack of comprehensive comparative research focused on timber bridges, particularly those using CLT. Accordingly, this study aims to assess the feasibility of utilizing CLT panels manufactured from locally sourced New Zealand Radiata Pine in bridge construction. Figure 2 provides a few examples of CLT panel applications in bridge contexts.

[1] Reza Masoudnia, PhD in Timber Structural Engineering, Honorary Lecturer at the University of Waikato, Senior Timber Structural Engineer in Red Stag, Hamilton, New Zealand, reza.masoudnia@redstag.co.nz, reza.masoudniaa@gmail.com

 https://doi.org/10.52202/080513-0702

Structural analysis of the CLT panels showed they can withstand a load of 707 kg/m², which meets the requirements for pedestrian and bicycle bridges and is strong enough to support the weight of a light vehicle. Figure 3 displays the loading scenarios considered for CLT bridge designs.

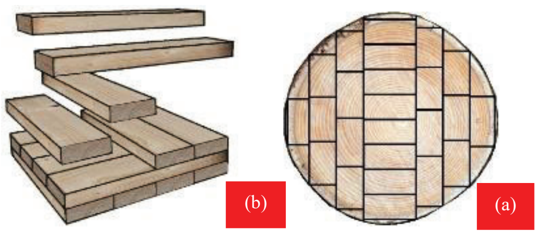

Figure 1. CLT production process; (a) Sawing log, (b) Arranging boards and final CLT product.

In addition, the reduced weight of CLT bridges and the benefits of off-site prefabrication contribute significantly to improved construction efficiency. Compared to concrete-steel composite bridges, CLT offers a renewable alternative that actively sequesters carbon throughout its life cycle. CLT bridges are not only lighter and stronger but also more environmentally sustainable, which helps shorten transportation times and accelerate on-site assembly (see Figure 4). Furthermore, through optimized prefabrication in the controlled setting of a CLT factory, most non-structural components of the bridge can be produced using surplus CLT material.

Recent studies on CLT panels show that they emit approximately 75% less carbon dioxide the main greenhouse gas driving human induced climate change compared to reinforced concrete across a range of conditions. By comparison, timber-concrete composite systems produce around 65% less CO_2, with their environmental benefits increasing as the span length grows [7].

The lightweight nature and prefabrication capabilities of CLT bridges can greatly accelerate and simplify the repair or replacement process. As illustrated in Figure 5, the bridge can remain partially operational during construction activities. Damaged sections of the CLT bridge can be swiftly replaced with new prefabricated components. Even elements such as the concrete topping and handrails can be pre-cast and assembled in advance, enabling faster reopening and a quicker return to full functionality. Additionally, the use of an upside-down wide spline joint can make the reassembly process considerably easier, faster, and safer minimizing disruption to traffic flow.

Figure 2. CLT panel application for short-span bridges.

Large-scale fire testing of CLT panels currently available in the New Zealand market has shown that these panels are suitable for use in vehicle bridges. Under structural loading conditions, CLT panels can maintain their structural integrity for over 60 minutes during a fire event at 900 degrees Celsius (see Figure 6). Existing fire test data is derived from configurations designed for building applications, where the fire exposure occurs on the underside of the panel [10]. While no current fire test results are available for scenarios involving fire exposure on the top surface relevant for bridge applications it is anticipated that CLT panels would perform significantly better in such cases due to a notably lower charring rate. This key difference in charring behavior is illustrated in Figure 6, which shows a seven-layer CLT panel as an example.

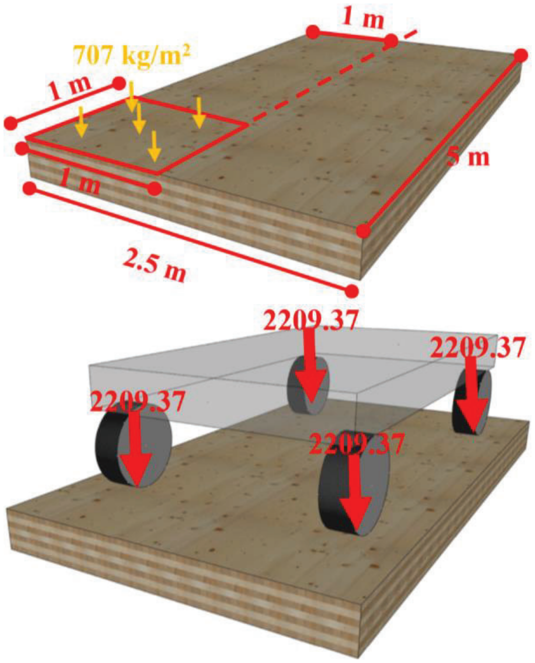

Figure 3. Uniformly loaded CLT bridge and equivalent loading for vehicle load configuration.

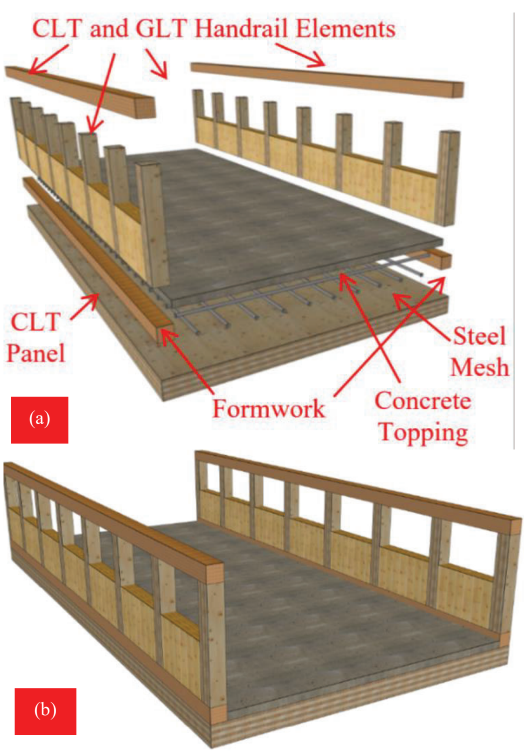

Figure 4. Prefabricated CLT bridge; a) before assembly, b) after assembly.

2- EXPERIMENTAL TEST SET-UP

A real-scale four-point bending test has been conducted on a single five-layer CLT panel with a width of 2000 mm, a thickness of 200 mm, and a length of 6000 mm using a Material Testing Systems (MTS) actuator testing machine to verify the structural performance of the panel (refer to Figure 7) [15]. The data acquisition system has the ability to record load data from the MTS, and three LVDTs were located on top of each of the two end supports and under the mid-span of the CLT panel at the same time, as shown in Figure 8.

The same test set-up has been used for testing CLT composite beam. The CLT panel is attached as top flange to the top of a LVL girder. The external top, bottom, and middle layers of the CLT panel were oriented in the longitudinal direction of the LVL beam assembly which was 302 mm wide, 610 mm deep and 7 meter long (refer to Figure 9).

The CLT slab was predrilled, and the two parts were mechanically fastened using 550-mm screws with a diameter of 11 mm. A total of 48 screws were used in the test to provide composite action between CLT slab and LVL beam. The screws penetrated the 200-mm CLT slab and entered the supporting LVL beam at a 45° angle to a depth of approximately 276 mm.

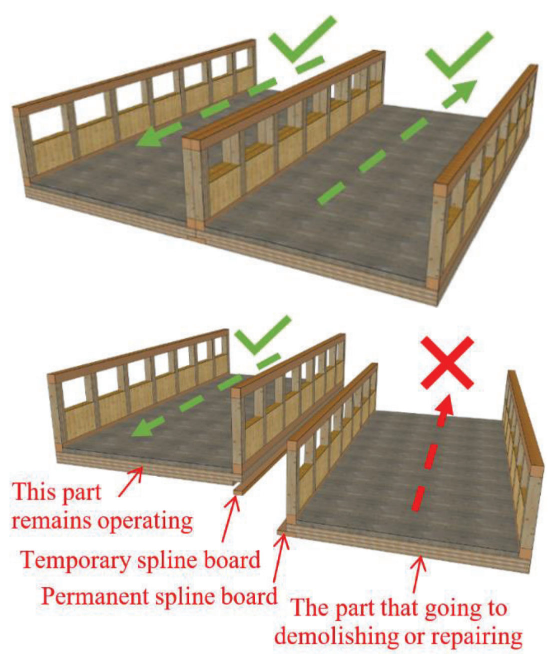

Figure 5. CLT bridge can remain semi-operational during the replacement of the old or damaged part of the bridge. a) fully operational, b) partially disassembled, and semi-operational.

https://doi.org/10.52202/080513-0702

3- NUMERICAL ANALYSIS

The finite element package ABAQUS version 6.13-3 was chosen for the analysis and simulation of a simply supported CLT panel in bending. The detailed numerical modelling and convergence study confirmed the accuracy of the developed numerical model (refer to Figures 10 and 11). An eight-node element (C3D8R), which is a linear three-dimensional solid element, was used for the analysis of the CLT panel [12-15]. The CLT properties specified in this study are for timber boards made from Radiata Pine trees grown commercially in New Zealand (refer to table 1). The coordinate system used is based on the principal axes of the wood , as shown in Figure 12.

Figure 6. Red Stag CLT fire test.

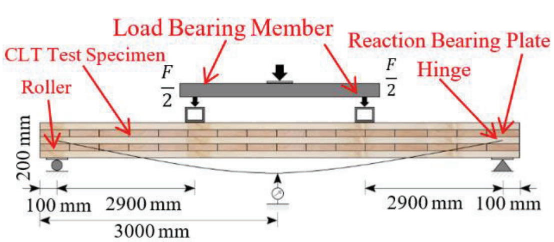

Figure 7. Test set-up for measuring the modulus of elasticity [15].

3.1 CONVERGENCE STUDY

Convergence studies were carried out on the 6-meter CLT panel to find a suitable finite element mesh to increase the accuracy of the analysis. Figure 13 and 14 illustrate the mid- span deflection of the CLT panel that is plotted against the corresponding number of elements for ten different mesh sizes [15].

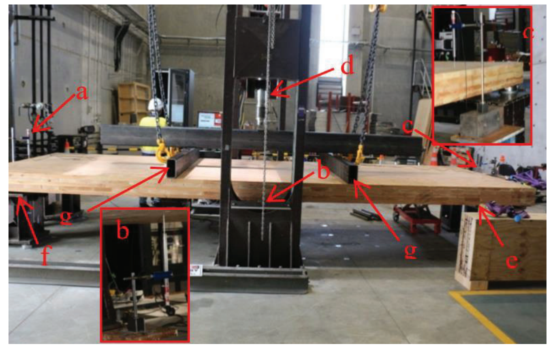

Figure 8. 500 kN MTS testing machine configured for four-point bending test. (a) LVDT 1, (d) MTS Machine, (e) Roller Support, (f) Hinge Support, (g) Load Bearing Plate, and (h) Data Acquisition System [15].

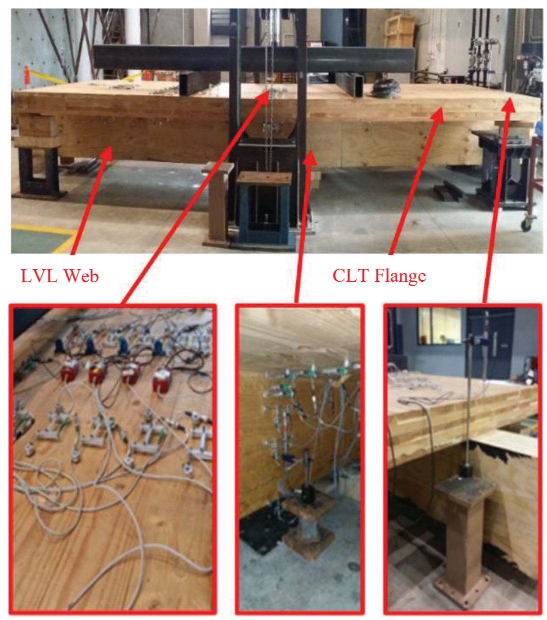

Figure 9. Experimental test set-up. (a) LVDT , (d) MTS Machine, (e) Roller Support, (f) Hinge Support, (g) Load Bearing Plate, and (h) Data Acquisition System [15].

Table 1. Material Properties of the CLT's boards [12-15].

Component	E_L	E_R	E_T	ν_{LT}	ν_{TL}	ν_{LR}	ν_{RL}	ν_{TR}	ν_{RT}
MSG 8 boards	8000	363	363	0.2	0.018	0.15	0.018	0.21	0.18
MSG 6 boards	6000	272	272	0.15	0.013	0.11	0.013	0.09	0.13

E=Modulus of Elasticity (N/mm2 for all modulus for CLT's boards).
v=Poison's ratio, L=Longitudinal, R=Redial, T=Tangential

4- PARAMETRIC STUDY AND RESULT DISCUSSION

The experimentally verified numerical model has been used to study the capability of various panel thicknesses for bridge applications (refer to Table 1). The mid-span deflection measurements show that the model is sufficiently accurate to predict the behaviour of the CLT panel.

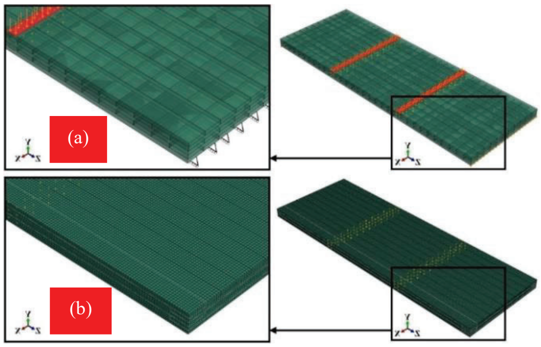

Figure 10. Typical boundary conditions and finite element mesh used in this study. (a) FE model boundary conditions (Load and support), (b) Finite element mesh.

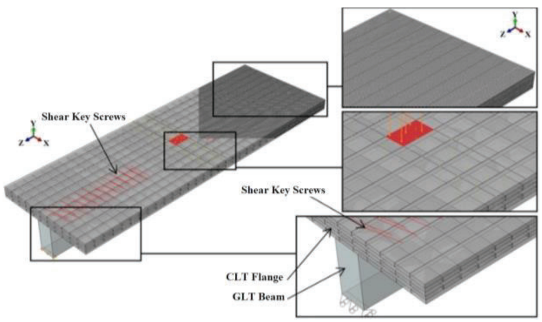

Figure 11. General arrangement of the numerical model to show boundary conditions and mesh.

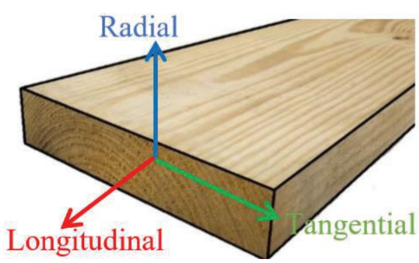

Figure 12. Principal axes of wood for numerical model.

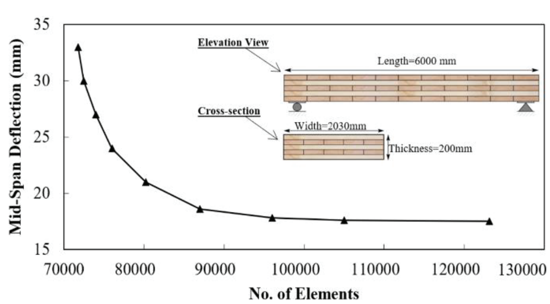

Figure 13. Convergence study numerical results.

Numerical analysis and analytical calculations have confirmed the structural capability of the CLT panels made from commercially grown New Zealand Radiata Pine trees for bridge applications. Specifications, shear, and moment capacity of various cross-section sizes of the CLT panel for bridge application are summarised in Table 3 to Table 4 [16-17].

The construction industry (including buildings and other types of structures) is a large contributor to greenhouse gas emissions and a massive consumer of natural resources. Therefore, even small improvements in construction technologies are important to reduce greenhouse gas emissions and thereby attain national goals to mitigate climate change. Table 5 presents long-term locked-up carbon for six CLT bridge configurations and their serviceability performance under 707 kg/m^2 [20]. The comparison between numerical and analytical calculations shows that the analytical calcination results are by 10% over design and conservative (refer to table 6).

Table 2. Comparison of the mid-span deflection results.

Specimen	CLT's Lamella $W^1 \times T^2 \times L^3$ (mm)	Deflection Experimental	Deflection Numeical
CLT Panel	2030×200×6000	18 mm*	17.9 mm*
W=Width, T=Thickness, L=Length of the CLT panel * Deflections under 50 kN four points loading test.			

Table 3. Specifications of the CLT panels specimen.

Specimen Number	CLT's Lamella $W^1 \times T^2 \times L^3$	CLT's Lamella E_{longi} E_{trans}
1	1000 mm×210 mm×4000 mm	8 GPa 6 GPa
2	1000 mm ×210 mm×4000 mm	8 GPa 8 GPa
3	1000 mm×228 mm×5000 mm	8 GPa 6 GPa
4	1000 mm×228 mm×5000 mm	8 GPa 8 GPa
5	1000 mm×228 mm×5500 mm	8 GPa 6 GPa
6	1000 mm×228 mm×6000 mm	8 GPa 8 GPa
W=Width, T=Thickness, L=Length of the CLT panel E_{longi}=MoE of longitudinal layers, E_{trans}=MoE of transverse layers		

5- NUMERICAL PARAMETRIC STUDY

The main focus of study is investigation of various CLT panel configurations on the EFW of single and CLT composite double T-beams.

Table 4. The capacity of the CLT Panels.

Specimen Number	CLT's Panel Weight	Vn (kN)	Mn (kNm)
1	420 kg	55.42	421.3
2	420 kg	55.42	421.3
3	570 kg	141.21	69.47
4	570 kg	141.21	69.47
5	808 kg	188,73	97.56
6	882 kg	188.73	97.56
Factors: Ø=0.85, k_1=0.8, k_4=1, k_6=1, k_9=1, k_{12}=1 Refer to NZSAS 1720. Load Case: 1.2 Dead Load + 1.5 Live Load.			

https://doi.org/10.52202/080513-0702

Table 5. The serviceability performance and estimated carbon dioxide of the CLT Panels.

Specimen Number	Mid-span Deflection	Estimated Carbon	Sequestered Carbon Dioxide
1	9.9 mm	168 tons	727 tons
2	9.4 mm	168 tons	727 tons
3	16.2 mm	228 tons	1048 tons
4	15.8 mm	228 tons	1048 tons
5	14.8 mm	323 tons	1487 tons
6	5.7 mm	352 tons	1622 tons
Mid-Span Deflection: Long-Term Deflection: (G+Ψl Q)×j2+(Ψs+Ψl)Q.			

Table 6. Mid-span deflection result based on experimentally verified numerical analysis.

Specimen Number	CLT's Lamella $W^1 \times T^2 \times L^3$ (mm)	CLT's Lamella $E_{longitudinal}$ $E_{transverse}$	Deflection Numeical
1	1000×210×4000	8 GPa 6 GPa	8.9 mm*
2	1000×210×4000	8 GPa 8 GPa	8.9 mm*
3	1000×228×5000	8 GPa 6 GPa	15.6 mm*
4	1000×228×5000	8 GPa 8 GPa	14.3 mm*
5	1000×228×5500	8 GPa 6 GPa	13.3 mm*
6	1000×228×6000	8 GPa 8 GPa	5.1 mm*
W=Width, T=Thickness, L=Length of the CLT panel $E_{longitudinal}$=MoE of longitudinal layers, $E_{transverse}$=MoE of transverse layers * Deflections under 50 kN four points loading test.			

5.1 EFFECT OF CLT PANEL LAYER CONFIGURATION

Two groups of single and double CLT composite beams with various CLT layers configurations were analysed to investigate the effect of layer thickness on the EFW. As seen from table 7 and Figure 13 (Specimens 2 to 1), an increase in the transverse layer thickness enhances the EFW. Again, numerical analysis result shows that similar increase in the transverse layer thickness over longitudinal layer enhances the EFW in double CLT composite beams (refer to table 8, Specimens 14 vs 13 and 12).

In the first series of analysis of CLT composite single T-beams, when 20 mm transverse boards in 166 thick CLT panel are replaced by 40-mm-thick boards, and the 20 mm thick, EFW increased 210 mm (Configuration 2 and 1 in Table 3). Moreover, when the 40-mm longitudinal layers and 20-mm transverse layers in Configurations 3 were replaced by boards with a thickness of 40 mm and 20 mm (Configurations 1 in table 7), the EFW increased more than 4 times. The similar change in CLT composite double T-beam increasing the CLT slab effective width noticeably more than 4.7 times (Configuration 14 and 15 in table 8). Therefore, the space between two LVL girders in the CLT composite double T-beam could be increased by 1500 mm based on the predicted EFW of the CLT composite double T-beam.

5.2 EFFECT OF CLT MATERIAL PROPERTIES

The effect of the elastic modulus of the CLT panels on the EFW are provided in Figure 15, 16, Table 7 and 8. In general, increasing the modulus of elasticity of the CLT panels increased the EFW of Single and double CLT composite T-beams. For example, as shown in Figure 15, when the modulus of elasticity of the CLT panel increased from 6 GPa (Configuration 5 in Table 7) to 8 GPa (Configuration 1 in Table 7), the EFW increased from 760 to 790 mm, thus increasing by 5 and 30%, respectively.

In addition, the comparison indicates when the 6 GPa transverse boards in 210 mm thick CLT panels in single and double CLT composite beams replaced with 8-GPa boards, EFW enhances 85 mm and 180 mm respectively. The numerical parametric analysis showed that higher ratio of longitudinal thickness over transverse layer has higher improvement effect on EFW compared to higher ratio of longitudinal MoE over transverse layer MoE.

It is really important to note all these numerical analyses are only practicing the EFW of single or double CLT composite beams and the CLT slab required further deign and investigation based on structural application.

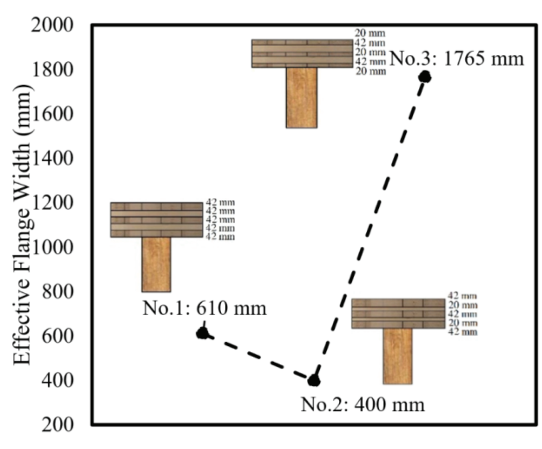

Figure 13. Effect of the layer's configuration change on the effective flange width for Configurations 1, 2, 3.

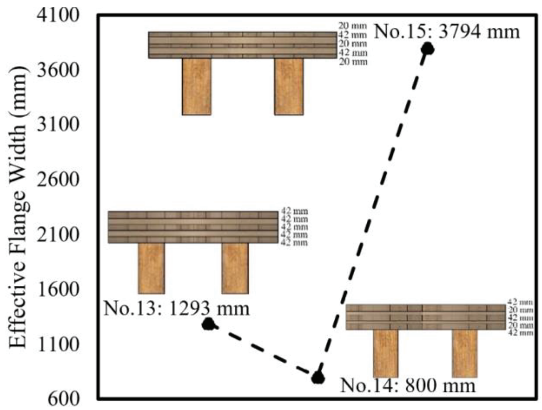

Figure 14. Effect of the layer's configuration change on the effective flange width for Configurations 13, 14, 15.

For instance, the 3-layer central layers of 5-layer CLT panel in CLT composite double T-beam should be design as simply supported CLT panel to ensure the system can perform structurally safe for floor application. The Figure 18 and Table 8 shows that how high loads due to heavy vehicle weights on CLT panel between side-by-side girders lead to reduction girders spacing in CLT composite double T-beams.

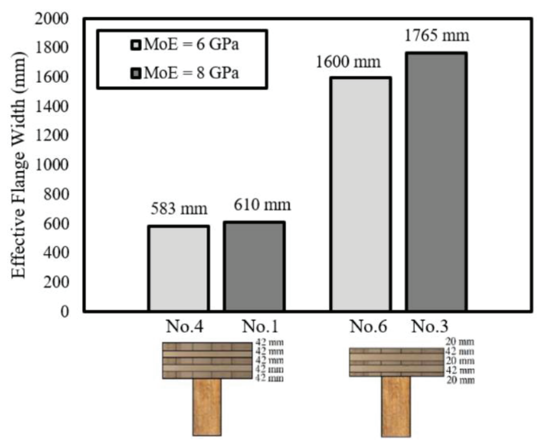

Figure 15. Effect of CLT material properties on effective flange width of CLT composite single T-beams.

6- CONCLUSIONS

An accurate numerical model has been developed, which has been experimentally verified. The numerical parametric study and analytical calculations show that the bare CLT panel and CLT composite double T- beams are sufficiently strong to carry structural loads for various bridge applications.

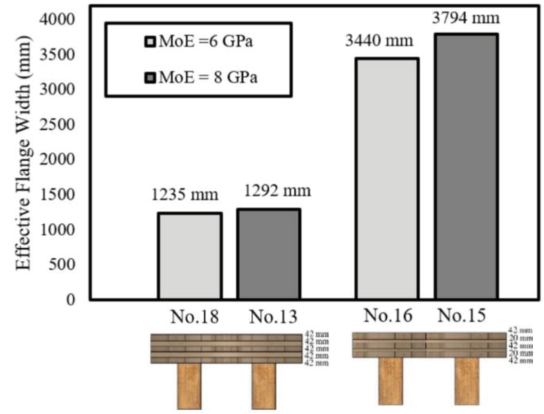

Figure 16. Effect of CLT material properties on effective flange width of CLT composite double T-beams.

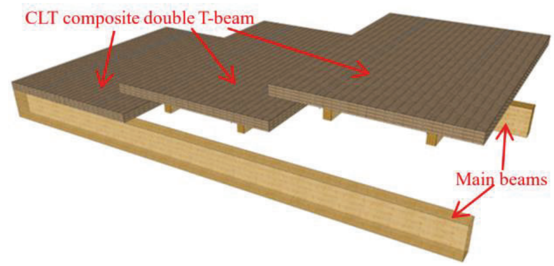

Figure 17. Intermediate Span CLT composite double T-beams.

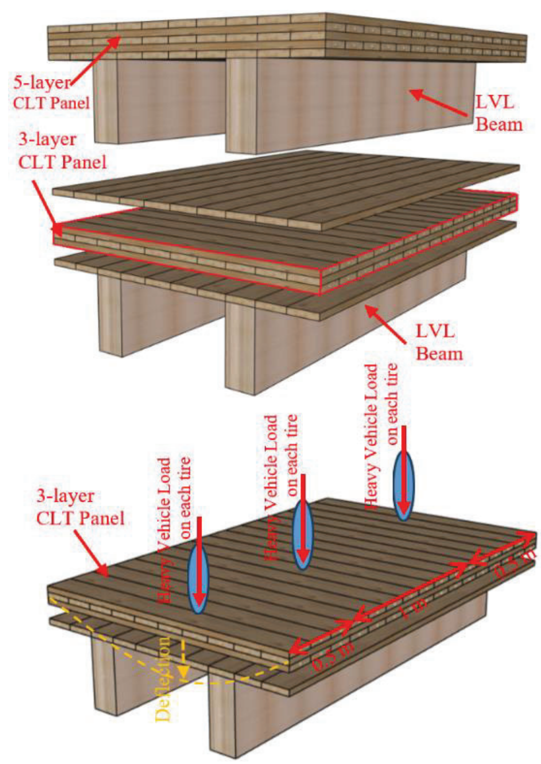

Figure 18. CLT composite double T-beam structural design concept for bridge application.

https://doi.org/10.52202/080513-0702

Table 7. CLT composite T-beam specifications and EFW result.

Specimen Number	CLT W×T×L (mm)	CLT MoE of Layers (GPa)	LVL W×T×L (mm)	LVL MoE (GPa)	Predicted effective width flange (mm)
1	2000×210×6000 2000×(42+42+42+42+42)[a]×6000	8,8,8,8,8 [b]	350×600×6000	11	610
2	2000×166×6000 2000×(42+20+42+20+42)[a]×6000	8,8,8,8,8 [b]	350×600×6000	11	400
3	2000×166×6000 2000×(20+42+20+42+20)[a]×6000	8,8,8,8,8 [b]	350×600×6000	11	1765
4	2000×210×6000 2000×(42+42+42+42+42)[a]×6000	6,6,6,6,6 [b]	350×600×6000	11	583
5	2000×166×6000 2000×(42+20+42+20+42)[a]×6000	6,6,6,6,6 [b]	350×600×6000	11	380
6	2000×166×6000 2000×(20+42+20+42+20)[a]×6000	6,6,6,6,6 [b]	350×600×6000	11	1600
7	2000×210×6000 2000×(42+42+42+42+42)[a]×6000	8,6,8,6,8 [b]	350×600×6000	11	570
8	2000×166×6000 2000×(42+20+42+20+42)[a]×6000	8,6,8,6,8 [b]	350×600×6000	11	365
9	2000×166×6000 2000×(20+42+20+42+20)[a]×6000	8,6,8,6,8 [b]	350×600×6000	11	1660
10	2000×210×6000 2000×(42+42+42+42+42)[a]×6000	6,8,6,8,6 [b]	350×600×6000	11	623
11	2000×166×6000 2000×(42+20+42+20+42)[a]×6000	6,8,6,8,6 [b]	350×600×6000	11	407
12	2000×166×6000 2000×(20+42+20+42+20)[a]×6000	6,8,6,8,6 [b]	350×600×6000	11	1810

Note: MoE = modulus of elasticity (units of GPa).
[a] Numbers in parentheses are the thickness of individual CLT layers (units of mm).
[b] The five numbers are the modulus of elasticity of each layer (units of GPa).
W: Width, T: Thickness, L: Length (units of mm).

Table 8. CLT composite double T-beam specifications and EFW result.

Specimen Number	CLT W×T×L (mm)	CLT MoE of Layers (GPa)	LVL W×T×L (mm)	LVL MoE (GPa)	Predicted EFW (mm)	Practical EFW for Bridge Application
13	4000×210×6000 4000×(42+42+42+42+42)[a]×6000	8,8,8,8,8 [b]	Two 350×600×6000	11	1293	798 mm
14	4000×166×6000 4000×(42+20+42+20+42)[a]×6000	8,8,8,8,8 [b]	Two 350×600×6000	11	800	Not Applicable
15	4000×166×6000 4000×(20+42+20+42+20)[a]×6000	8,8,8,8,8 [b]	Two 350×600×6000	11	3794	683 mm
16	4000×210×6000 4000×(42+42+42+42+42)[a]×6000	6,6,6,6,6 [b]	Two 350×600×6000	11	1235	700 mm
17	4000×166×6000 4000×(42+20+42+20+42)[a]×6000	6,6,6,6,6 [b]	Two 350×600×6000	11	760	Not Applicable
18	4000×166×6000 4000×(20+42+20+42+20)[a]×6000	6,6,6,6,6 [b]	Two 350×600×6000	11	3440	632 mm
19	4000×210×6000 4000×(42+42+42+42+42)[a]×6000	8,6,8,6,8 [b]	Two 350×600×6000	11	1208	704 mm
20	4000×166×6000 4000×(42+20+42+20+42)[a]×6000	8,6,8,6,8 [b]	Two 350×600×6000	11	730	Not Applicable
21	4000×166×6000 4000×(20+42+20+42+20)[a]×6000	8,6,8,6,8 [b]	Two 350×600×6000	11	3569	697 mm
22	4000×210×6000 4000×(42+42+42+42+42)[a]×6000	6,8,6,8,6 [b]	Two 350×600×6000	11	1410	797 mm
23	4000×166×6000 4000×(42+20+42+20+42)[a]×6000	6,8,6,8,6 [b]	Two 350×600×6000	11	814	Not Applicable
24	4000×166×6000 4000×(20+42+20+42+20)[a]×6000	6,8,6,8,6 [b]	Two 350×600×6000	11	3891	699 mm

Note: MoE = modulus of elasticity (units of GPa).
[a] Numbers in parentheses are the thickness of individual CLT layers (units of mm).
[b] The five numbers are the modulus of elasticity of each layer (units of GPa).
W: Width, T: Thickness, L: Length (units of mm).

https://doi.org/10.52202/080513-0702

This study demonstrates that the high strength-to-weight ratio of CLT panels provides a lightweight, sturdy bridging solution for short-span bridges. In addition to their exceptional strength, CLT panels, as a mass timber material, also exhibit high dimensional stability. This ensures that bridges constructed from seven layers or thicker CLT panels, comprised of treated timber boards and protected with a waterproof membrane and concrete topping, can resist distortion even in extreme weather conditions, further improving their service life. The numerical parametric study of single and double CLT composite T-beams shows that the EFW increases with any change that increases the ratio of transverse layer depth to longitudinal layer depth.

Moreover, using thicker longitudinal layers in CLT slabs of similar thickness decreased the effective flange width. Furthermore, stiffer transverse layers in CLT panels with a higher modulus of elasticity slightly improved the EFW. structural design performance check of the CLT panel perpendicular to LVL Girder reveals the spacing restrictions of LVL girders due to high loads of heavy vehicles weight. Finally, the installation of a CLT bridge is much faster due to its lighter weight, making it a great substitute for a concrete bridge. This helps replace a carbon-intensive material with a renewable, low-carbon alternative.

ACKNOWLEDGEMENT

The author thanks graphic designer Nariman Valizadeh and Navid Masoudnia for providing excellent photos and figures. I would also like to thank Red Stag for financially sponsoring this research paper.

This technical paper has been developed to demonstrate the significant structural potential of CLT panels and CLT composite double T-beams constructed from Red Stag CLT panels for bridge applications. Please note that it is the responsibility of the bridge engineer or designer to ensure that the presented results are appropriate for their specific project and not to rely solely on the numerical analyses.

REFERENCES

[1] A. Fortune, P. Quenneville. Feasibility study of New Zealand radiata pine cross-laminated timber, New Zealand Timber Design Journal, 2011.

[2] M. Mohammad, S. Gagnon. Introduction to Cross-Laminated Timber, Wood Design Focus, Volume 22, Number 2, pp. 13-21; 2012

[3] B. Yeh, S. Gagnon, T. Williamson, C. Pirvu, C. Lum, D. Kretschmann, The North American Product Standard for Cross-Laminated Timber, Wood Design Focus, Volume 22, Number 2, pp. 13-21; 2012.

[4] M. Jelec, D. Varevac, V. Rajcic, Cross-laminated timber (CLT) - A state of the art report, GRADEVINAR, 70 (2), 75-95.

[5] R. Brandner, G. Flatscher, A. Ringhofer, G. Schickhofer, A. Thiel, Cross laminated timber (CLT): overview and development, Wood and Wood Products, Volume 74, pages 331–351, (2016).

[6] K. Lewis, R. Shrestha, K.I. Crews, Introduction to cross-laminated timber and development of design procedures for Australia and New Zealand, 23rd Australasian Conference on the Mechanics of Structures and Materials (ACMSM23), 2014.

[7] M. F. Laguarda Mallo, O, Espinoza, Cross-laminated timber vs. Concrete/steel: cost comparison using a case study, World Conference on Timber Engineering 2016, Vienna, Austria.

[8] S. Ahmed, I. Arocho, Analysis of cost comparison and effects of change orders during construction: Study of a mass timber and a concrete building project, Volume 33, Journal of Building Engineering January 2021, 101856.

[9] M. F. Laguarda Mallo, O, Espinoza, Outlook for Cross-Laminated Timber in the United States, bioresources 2014, 10.15376/biores.9.4.7427-7443.

[10] Red Stag CLT Design Guide V1.5, September 2024.

[11] P. Maclaren. Radiata Pine Growers Manual. New Zealand Forest Research Institute, Rotorua, New Zealand, 1993.

[12] R. Masoudnia, A. Hashemi, and P. Quenneville. “Predicting the effective flange width of a CLT slab in timber composite beams.” In: Journal of Structural Engineering 144.7 (2018), pp. 04018084.

[13] R. Masoudnia, A. Hashemi, and P. Quenneville. “Evaluation of effective flange width in timber composite beams.” In: New Zealand Timber Design Journal 26.2 (2018), pp. 14–24.

[14] R. Masoudnia and S. Masoudnia. “Numerical investigation of effective flange width in CLT-GLT composite T-beams.” In: New Zealand Timber Design Journal 27.3 (2019), pp. 7–16.

[15] R. Masoudnia. “State of the art of the effective flange width for composite T-beams.” In: Construction and Building Materials 244 (2020), Art. 118303.

https://doi.org/10.52202/080513-0702